

A Compensated Acoustic Actuator for Systems with Strong Dynamic Pressure Coupling

Charles Birdsong and Clark J. Radcliffe

Department of Mechanical Engineering
Michigan State University
East Lansing, MI 48824-1229

ABSTRACT

Audio speakers are commonly used as acoustic actuators for noise control applications. Recent developments in the use of compensated dual-coil speakers have improved the performance of these acoustic actuators. However, the performance of these speakers depends on the application. When they are applied in systems with strong coupling between the plant and the actuator, the velocity sensor used in previous work must be improved.

This study considers the application of a compensated speaker as an actuator. An acoustic duct is used as an example of a plant that exhibits strong dynamic pressure interaction with the actuator. The speaker dynamics and the acoustic duct dynamics are first modeled separately. The two systems are then coupled, and the resulting system is modeled. A velocity sensor is developed and used in feed-back compensation. The resulting speaker system behaves as an ideal actuator with minimal magnitude and phase variation over a 0 – 200 Hz bandwidth. These conclusions are verified through experimental results.

This study is important in the overall area of acoustic actuators and active noise control. The actuator developed here will significantly aid in the goal of active noise control in an acoustic duct.

INTRODUCTION

Active noise control is an expanding field in the automotive and aircraft industries. Commercial products are currently available to create quiet interior spaces [Bradley 1995, Warner 1995]. These systems use passive and active controls to treat unwanted noise. Passive control consists of applying dampening material to treat high frequency noise. Dampening material must be of the same physical dimension as the wavelength of the sound wave to be effective [Radcliffe, et al, 1994]. Below 200 Hz the wave length in air is approximately 0.26 m or longer. This would require an unrealistic amount of dampening material approximately one quarter of a meter thick for effective passive noise control. For low frequency noise, active controls methods can be used. Active control relies on a combination of sensors, a controller, and actuators to treat noise in the system (plant).

One system that has received much attention in this field is the acoustic duct, which consists of a long, hard walled enclosure. Hull showed that the resonances excited by a noise source in an acoustic duct can be attenuated using feedback active noise control [Hull 1993]. Attempts at wide band noise control were hindered by actuator dynamics that caused the measured control input to deviate from the desired control.

Gogate proposed a strategy for eliminating the effects of speaker dynamics through feed-back compensation [Radcliffe et al. 1996]. The original design did not include the effects of the coupled dynamics through the interaction of the plant pressure and the actuator. Figure 1 shows the speaker face velocity to primary coil voltage frequency response of the original compensator with two cases: the dashed line represents the response of the speaker in free-air, and the solid line represents the response when the speaker is coupled with an acoustic duct. In free-air there is little magnitude and phase variation from 0 - 200 Hz. When the speaker is coupled with the acoustic duct, there are large magnitude and phase variations exhibited at the resonance frequencies of the duct.

The original compensator fails to eliminate the dynamics associated with the duct.

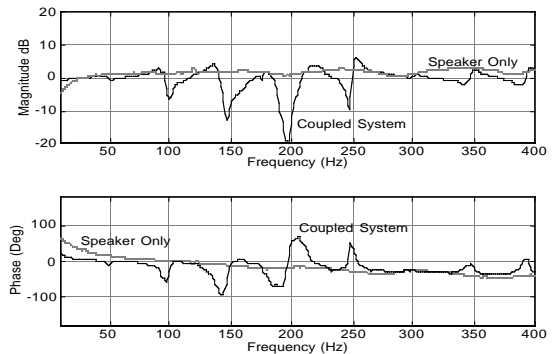


Figure 1: Speaker Face Velocity to Primary Coil Voltage Using Original Compensator

This study presents an acoustic actuator that compensates for both actuator and plant dynamics. The acoustic duct is presented as a plant in order to demonstrate the robustness of the system to a plant with strong coupling with the actuator through pressure interaction. A model of a dual voice-coil speaker is first presented, and a velocity sensor is developed. It is shown that the speaker dynamics can be eliminated through feed-back compensation. A model of an acoustic duct is presented next, which predicts the pressure response due to a velocity input. Finally, the two systems are coupled, and it is shown that the speaker compensation minimizes both the speaker and the acoustic duct dynamics through feed-back compensation. The results in every stage of the modeling and analysis are verified through experimental testing, and model results are presented together with experimental results. Figure 2 shows the experimental setup used to verify the model results.

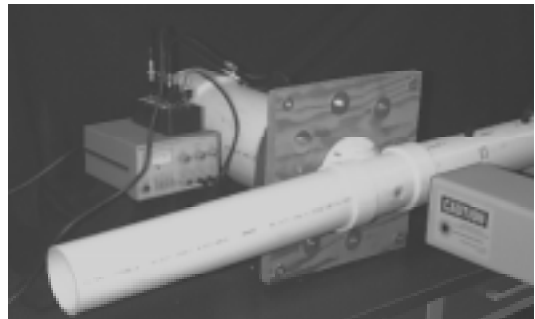


Figure 2: Acoustic Duct and Compensated Actuator Setup

The work presented here provides a method for creating an ideal acoustic actuator for systems that include strong plant and actuator coupling and brings the goal of active noise control of systems such as the acoustic duct one step closer.

ACOUSTIC ACTUATOR SPEAKER MODEL

Audio speakers are commonly used as acoustic actuators in noise control systems. They are beneficial because a small voltage applied to a speaker can generate a strong control effort. Audio speakers are relatively inexpensive and widely available in commercial sizes and models. Speakers have the disadvantage that the response of a speaker can be strongly affected by both the dynamics associated with the free-air resonance of the speaker and the dynamics of the system it is driving. An ideal actuator will have a pure gain over the required bandwidth. When a speaker is affected by dynamics, it can exhibit significant magnitude and phase variations limiting its performance. If a speaker is to be used as an acoustic actuator, these effects must be minimized.

One method of minimizing magnitude and phase variations is to apply feedback compensation to the speaker. If the speaker response can be measured, then the signal can be applied to a feedback controller, the response can be driven to the desired output, and the magnitude and phase variation can be reduced. An accurate speaker face velocity sensor is therefore required.

One variety of speaker named the “dual voice-coil” speaker has certain characteristics that make it ideal for use as an acoustic actuator [Radcliffe et al., 1996]. The dual voice-coil speaker has 2 independent wire coils intertwined and wrapped around a bobbin which is allowed to slide over a permanent magnet. This configuration is shown in Figure 3.

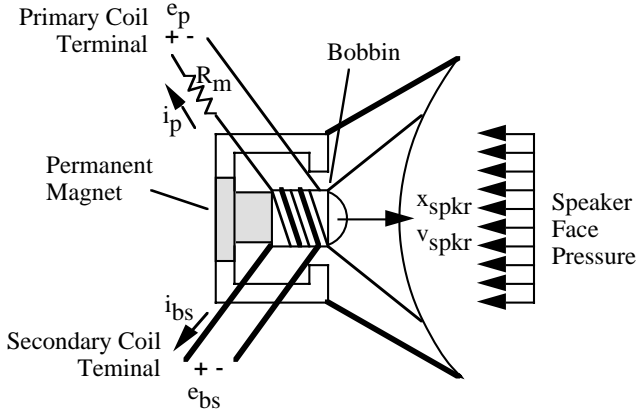


Figure 3: Dual Voice-Coil Speaker Diagram

A transfer function model of the system can be developed which relates the inputs: primary coil voltage, secondary coil current and speaker face pressure to the outputs: secondary coil voltage, primary coil current and speaker face velocity [Birdsong, 1996]. An infinite impedance is applied to the secondary coil forcing the current to zero, eliminating the secondary current as an input.

The speaker parameters necessary to define the model are the mechanical inertia of speaker, I_{spkr} ; mechanical compliance of speaker, C_{spkr} ; viscous friction of speaker, R_{spkr} ; electromagnetic coupling factor, bl ; speaker coil resistance, R_{coil} ; the current sensing resistor resistance, R_m ; speaker coil inductance, I_{coil} ; mutual inductance, M_{coil} ; and the equivalent speaker area, S_D . With the exception of mutual inductance, M_{coil} , these electrical and mechanical parameters are defined in IEEE standard 219-1975 [IEEE Standard 219-1975] for loudspeaker measurements.

The transfer function model of the system is given by

$$\begin{pmatrix} e_{bs}(s) \\ i_p(s) \\ v_{spkr}(s) \end{pmatrix} = \begin{bmatrix} G_{ebs/ep} & G_{ebs/p} \\ G_{ip/ep} & G_{ip/p} \\ G_{vspkr/ep} & G_{vspkr/p} \end{bmatrix} \begin{pmatrix} e_p(s) \\ P(s) \end{pmatrix} \quad (1)$$

Each element in the transfer function matrix $G(s)$ is given by

$$G_{ebs/ep} = \frac{C_{spkr} M_{coil} \left[I_{spkr} s^3 + R_{spkr} s^2 + \left(\frac{bl^2}{M_{coil}} + \frac{1}{C_{spkr}} \right) s \right]}{G_{den}} \quad (2)$$

$$G_{ip/ep} = \frac{[(C_{spkr} I_{spkr}) s^2 + (C_{spkr} R_{spkr}) s + 1]}{G_{den}} \quad (3)$$

$$G_{vspkr/ep} = \frac{[(bl C_{spkr}) s]}{G_{den}} \quad (4)$$

$$G_{ebs/p} = \frac{[-bl C_{spkr} S_D [(I_{coil} - M_{coil}) s^2 + R_{coil} s]]}{G_{den}} \quad (5)$$

$$G_{ip/p} = \frac{[(bl S_D C_{spkr}) s]}{G_{den}} \quad (6)$$

$$G_{vspkr/p} = \frac{[-S_D C_{spkr} [I_{coil} s^2 + R_{coil} s]]}{G_{den}} \quad (7)$$

and the denominator of the $G(s)$ matrix is given as

$$G_{den} = (C_{spkr} I_{spkr} I_{coil}) s^3 + (C_{spkr} I_{spkr} R_{coil} + C_{spkr} I_{coil} R_{spkr}) s^2 + (bl^2 C_{spkr} + I_{coil} + C_{spkr} R_{coil} R_{spkr}) s + R_{coil} \quad (8)$$

Equations (4) and (7) are new and important results not used in previous work. All of the speaker model transfer function equations will be useful when designing a velocity sensor for the speaker and when modeling the speaker coupled with the acoustic duct.

Velocity Feedback Compensation of Speaker

The velocity of the speaker, v_{spkr} , is strongly affected by the dynamics of the speaker and the pressure input, P . These effects will combine to create magnitude and phase variations in the primary coil voltage to speaker velocity response. One method of eliminating these unwanted effects is to apply a proportional feedback controller as shown in Figure 4. The transfer function for this system is given by (9), where K_p is the proportional gain and $H(s)$ is a velocity sensor. If the sensor transfer function is a real constant, k , over the controller bandwidth, then the closed loop transfer function, $T(s)$, will approach a constant, $1/k$ with zero phase. This compensation forces the speaker cone velocity to accurately follow the desired velocity input. The result is independent of the speaker dynamics and the input pressure provided that the sensor has a constant transfer function over the controller bandwidth.

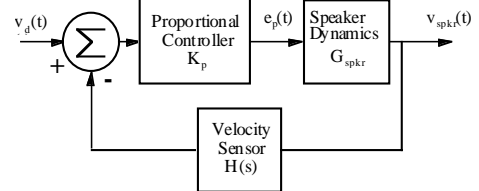


Figure 4: Proportional Feedback Controller

$$T_{spkr}(s) = \frac{V_{spkr}(s)}{V_d(s)} = \frac{K_p G_{spkr}(s)}{1 + K_p G_{spkr}(s) H(s)} \quad (9)$$

As K_p is increased, the transfer approaches $1/H(s)$ and the magnitude and phase variation approaches zero. This approach assumes that the velocity of the speaker face can be measured. A speaker velocity sensor is therefore needed which accurately

predicts the speaker velocity in the presence of speaker and plant dynamics.

The relation between the speaker velocity and the two other measurable outputs (the secondary coil voltage, e_{bs} and the primary coil current, i_p) is given in (1). The speaker velocity, V_{spkr} can be solved for in terms of E_{bs} and I_p yielding,

$$V_{spkr}(s) = H_{bs}E_{bs}(s) - H_p(s)I_p(s) \quad (10)$$

where $H_{bs} = 1/bl$ and $H_p(s) = sM_{coil}/bl$.

The secondary coil voltage, E_{bs} , can be measured directly from the speaker coil; the primary coil current, I_p , can be determined from the voltage across the resistor, R_m ; and H_{bs} is a pure gain ($1/bl$). The term $H_p(s)$ is a differentiator transfer function because it contains an 's' in the numerator. Such a transfer function cannot be realized exactly, but an approximation $\hat{H}_p(s)$ can be used where

$$\hat{H}_p(s) = \frac{M_{coil}}{bl} \left(\frac{s}{s + p_1} \right) \quad (11)$$

where p_1 is a pole location selected such that $\hat{H}_p(s)$ approximates $H_p(s)$ over the controller bandwidth.

Feedback compensation can now be implemented using the signal from the velocity sensor to compute the error between the desired velocity and the sensor velocity and a proportional controller to drive the speaker velocity to the desired velocity. It should be noted that the development of the velocity sensor did not assume that the pressure at the speaker face was constant, as in previous work. This new velocity sensor includes the effects of pressure as an input to the system. As a result, the closed-loop system minimizes magnitude and phase variations from not only the speaker dynamics (as in previous work) but in addition, the dynamics associated with the acoustic system, coupled through the pressure interaction with the speaker are minimized as well. This improvement over the previous velocity sensor is essential for the speaker to perform as an ideal actuator in a coupled system such as the acoustic duct.

ACOUSTIC DUCT SYSTEM MODEL

The acoustic duct is a system that exhibits strong dynamics that when coupled with the speaker system will cause large magnitude and phase variations in the speaker response. These effects can then be minimized through feed-back compensation. A mathematical model is needed for the acoustic duct before these effects can be demonstrated.

In this section, a model that accurately represents the duct pressure response is developed. System equations are first presented, then they are transformed into state space and transfer function representations. The model is then verified by comparing it with experimental results obtained from an acoustic duct.

System Model

An accurate system model of the acoustic duct is needed for modeling, analysis. The linear second order wave equation modeling particle displacement in a hard-walled, one-dimensional duct is [Seto 1971, Doak 1973]

$$\frac{\partial^2 u(x,t)}{\partial t^2} - c^2 \frac{\partial^2 u(x,t)}{\partial x^2} = -\frac{\partial}{\partial x} \left[\frac{\delta(x)P(t)}{\rho} \right] - \sum_{i=1}^k [\delta(x-x_i)] \frac{\partial}{\partial t} \left[\frac{M_i(t)}{\rho S} \right] \quad (12)$$

where $u(x,t)$ = particle displacement, c = wave speed (m/s), x = spatial location (m), t = time (s), ρ = density of the medium (kg/m^3), $M_1(t)$ = mass flow input in the domain (kg/s), x_1 = location of mass flow input (m), S = speaker area driving the mass

flow input (m^2), $P(t)$ = pressure excitation at $x = 0$ (N/m^2), and $\delta(x)$ = the Dirac delta function. The partially reflective boundary condition at location $x = L$ is the relationship between the spatial gradient and the time gradient of the particle displacement and is expressed as [Seto 1971, Spiekerman 1986]

$$\frac{\partial u}{\partial x}(L,t) = -K \left(\frac{1}{c} \right) \frac{\partial u}{\partial t}(L,t); \quad K \neq 0 + 0i, 1 + 0i, \infty \quad (13)$$

where K = complex impedance of the termination end (dimensionless). The duct end at $x = 0$ is modeled as a totally reflective end. This boundary condition is

$$\frac{\partial u}{\partial x}(0,t) = 0 \quad (14)$$

which corresponds to an open duct end. The acoustic pressure of the system is related to the spatial gradient of the particle displacement by [Seto 1971]

$$P(x,t) = -\rho c^2 \frac{\partial u}{\partial x}(x,t) \quad (15)$$

The above four equations represent a mathematical model of the duct.

State Space Representation

To derive the state equations used throughout the analysis, separation of variables is applied to the unforced version of (12), (13) and (14). Solving for the separation constant and the eigenfunctions yields [Spiekerman 1990]

$$\lambda_n = \frac{1}{2L} \log_e \left(\frac{1-K}{1+K} \right) - \frac{n\pi i}{L}, \quad n = 0, \pm 1, \pm 2, \dots \quad (16)$$

$$\phi_n(x) = e^{\lambda_n x} + e^{-\lambda_n x} \quad (17)$$

where λ_n are the natural frequencies and $\phi_n(x)$ are the eigenfunctions of the duct. For a duct with one mass flow rate as the input, the above equations can be manipulated such that the following state space representation is produced [Hull,1990]:

$$\dot{a}(t) = A_{duct} a(t) + B_{duct} m(t) \quad (18)$$

where $a(t)$ = the vector of modal wave amplitudes

A_{duct} = the diagonal matrix $[c\lambda_n]$

B_{duct} = the matrix $\left\{ \left[\frac{1}{4c\lambda_n^2 L \rho S} \right] \frac{d\phi_n(x_i)}{dx} \right\}$

and $m(t)$ = the mass flow input $\frac{\partial M}{\partial t}$

The system output is the pressure at any position in the duct

$$P(x_m, t) = C_{duct}^T a(t) \quad (19)$$

where $P(x_m, t)$ = the pressure in the duct at $x = x_m$,

and C_{duct} = the column vector $\left[-\rho c^2 \frac{d\phi_n(x_m)}{dx} \right]$.

Equations (18) and (19) represent the state space formulation of the acoustic duct with complex impedance, K , on the termination end.

Duct Transfer Function

A velocity to duct pressure transfer function can be computed from the state space representation of the acoustic duct model for the case with one mass flow input. The transfer function representation will be used for the coupled speaker/duct system model.

The duct transfer function can be computed numerically from

$$G_{duct}(s) = \frac{P_{duct}}{m} = C_{duct}(sI - A_{duct})^{-1}B_{duct} \quad (20)$$

where sI is the Laplace variable times an identity matrix and $G_{duct}(s)$ is the speaker velocity to duct pressure transfer function. The mass flow rate, $m(t)$ can be replaced by the speaker face velocity, v_{spkr} , by the relation, $m(t) = S_D v_{spkr}(t)$, where S_D is the speaker area. The transfer function, $G_{duct}(s)$, will have a numerator which consists of a polynomial of order $2*n$ and a denominator of order $2*n+1$, where n is the number of modes in the model.

COUPLED SPEAKER-DUCT SYSTEM

In the previous discussions both the dynamics of a speaker and a duct were modeled separately. The model of the speaker assumed that the speaker face was exposed to atmospheric pressure. This implied that the speaker velocity was only affected by the primary speaker voltage. The model of the duct gave the pressure at a point in the duct given a velocity input.

These two systems can be coupled by allowing the velocity output of the speaker to be the input to the duct and the pressure output of the duct to be the input to the speaker. The velocity of the speaker face is then no longer affected only by the primary speaker voltage but also by the pressure generated in the duct, which must be determined from the coupled dynamics of the two systems. This coupling is illustrated by Figure 5.

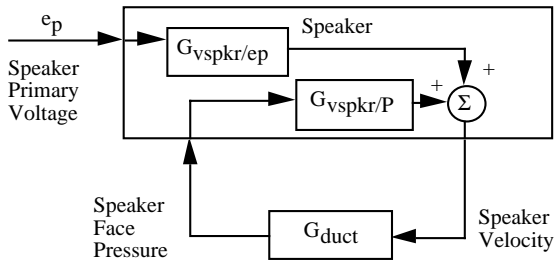


Figure 5: Coupled Speaker-Duct System

The coupled system can be modeled by combining the transfer functions of the speaker and duct models. The resulting transfer function can be used to model the open loop response of the coupled speaker-duct system. The speaker velocity, V_{spkr} is given by (1) as

$$V_{spkr}(s) = G_{vspkr/ep}(s)E_p(s) + G_{vspkr/P}(s)P(s) \quad (21)$$

The duct pressure to speaker velocity transfer function (20) is given by

$$\frac{P_{duct}}{V_{duct}} = G_{duct} \quad (22)$$

The pressure can be eliminated from (21) by substituting (22) which gives

$$V_{spkr}(s) = G_{vspkr/ep}(s)E_p(s) + G_{vspkr/P}(s)G_{duct}(s)V_{spkr}(s) \quad (23)$$

which can be solved for the transfer function of speaker velocity to primary speaker voltage as

$$\frac{V_{spkr}}{E_p} = \frac{G_{vspkr/ep}}{(1 - G_{vspkr/P}G_{duct})} \quad (24)$$

Velocity Sensor

The coupled system transfer function (24) can be used to model the response of the velocity sensor presented in the previous section. The velocity sensor model will include the effect of estimating the derivative of the primary current [Birdsong, 1996].

The secondary speaker voltage was given by (1). The pressure, P can be eliminated by replacing P with (22), giving

$$E_{bs}(s) = G_{ebs/ep}E_p + G_{ebs/P}G_{duct}V_{spkr} \quad (25)$$

The velocity can be eliminated replacing V_{spkr} with (24) giving the secondary speaker voltage to primary speaker voltage transfer function,

$$E_{bs}/E_p = G_{ebs/ep} + \left[\frac{G_{ebs/P}G_{vspkr/ep}G_{duct}}{(1 - G_{vspkr/P}G_{duct})} \right] \quad (26)$$

The primary speaker current, I_p is given by (1). The pressure and velocity can be eliminated as before, giving,

$$I_p/E_p = G_{ip/ep} + \left[\frac{G_{ip/P}G_{vspkr/ep}G_{duct}}{(1 - G_{vspkr/P}G_{duct})} \right] \quad (27)$$

The transfer functions (26) and (27) can be substituted into the velocity sensor equation (10) to give the sensor velocity to primary speaker voltage transfer function as,

$$V_{sensor}/E_p = \frac{-M_{coil}s}{bl(s + p_1)} \left[G_{ip/ep} + \frac{G_{ip/P}G_{vspkr/ep}G_{duct}}{(1 - G_{vspkr/P}G_{duct})} \right] + \frac{1}{bl} \left[G_{ebs/ep} + \frac{G_{ebs/P}G_{vspkr/ep}G_{duct}}{(1 - G_{vspkr/P}G_{duct})} \right] \quad (28)$$

Equation (28) can be used to simulate the sensor velocity response of the coupled system.

The feedback compensation strategy can be applied to the coupled system. The sensor velocity accounts for the pressure input as well as the primary voltage input, and the closed-loop system compensates for the dynamics associated with both the speaker and the duct.

COUPLED SPEAKER-DUCT MODEL VERIFICATION

The coupled speaker/duct system model was verified through experimental testing. The speaker velocity model was first compared to experimental results, then the velocity sensor was shown to accurately predict the measured velocity. Finally, the velocity sensor was used in feedback compensation.

Speaker Velocity Model

The speaker/duct system was setup as shown in Figure 6. The speaker velocity to primary coil voltage transfer function was then measured using a Hewlett Packard Signal Analyzer model 35660A from 0 - 200 Hz. The speaker face velocity was measured using a Bruel & Kjaer Laser Doppler Velocity-Transducer Set Type 3544.

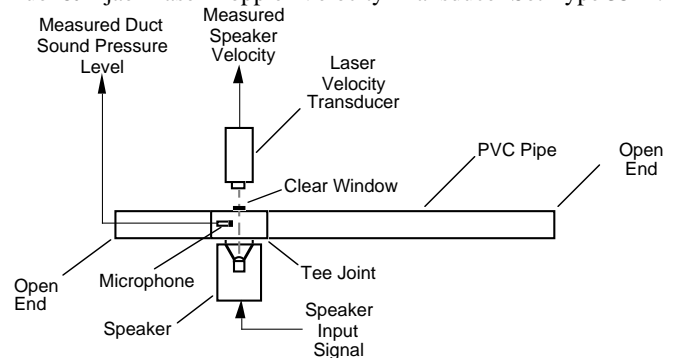


Figure 6: Experimental Acoustic Duct System

The model given by (24) was then used to compute the model response. Figure 7 shows the model response compared to the

measured response. The model response is shown by the solid line and the measured response is shown by the dashed line. An end impedance of $0.125+0j$ was used in the model. Good agreement was obtained by the model. There is less than 5 dB magnitude difference and 20 degrees and phase difference below 400 Hz.

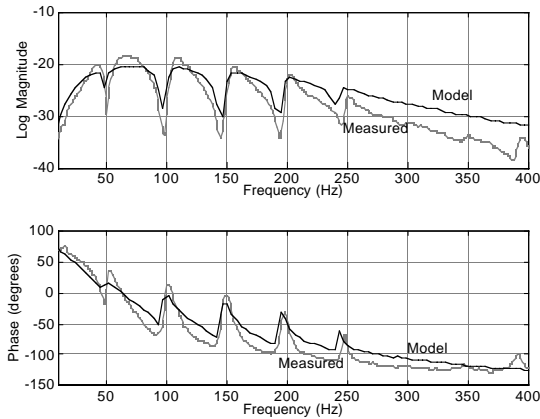


Figure 7: Comparison of Measured Frequency Response for Coupled Duct-Speaker System with Model

The resonances of the duct can clearly be seen in the speaker velocity response. These cause as large as 15 dB and 100 degrees of magnitude and phase variation. The free-air resonance of the speaker is also superimposed on the response. Clearly, the velocity of the speaker is affected by both the speaker and the duct dynamics.

For the application of active noise control of an acoustic duct, the objective is to attenuate the resonances in the duct. Figure 7 shows that the speaker response has the most error exactly where the control effort is needed, at the duct resonance frequencies. The response must be improved if the speaker is to be an effective acoustic actuator.

Velocity Sensor

The velocity sensor was then applied to the coupled speaker/duct system as show in Figure 8. A 2-inch foam plug was placed in the termination end to add damping to the system. An end impedance of $0.6+0.1j$ was used in the model.

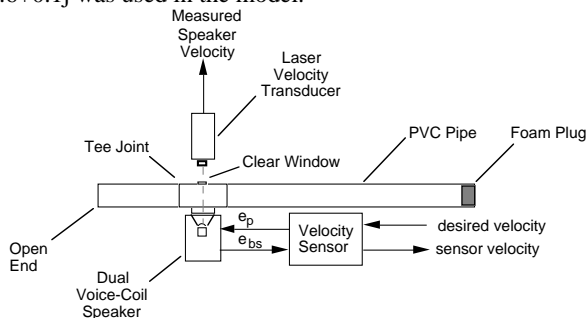


Figure 8: Diagram of Velocity Sensor in Speaker/Duct System Implementation

The sensor velocity to desired velocity and measured velocity to desired velocity transfer functions were then measured from 0 - 200 Hz using the signal analyzer. The modeled sensor velocity was also computed with (28) using the value of $p_1 = 1000$ Hz. Figure 9 shows good agreement between these three signals.

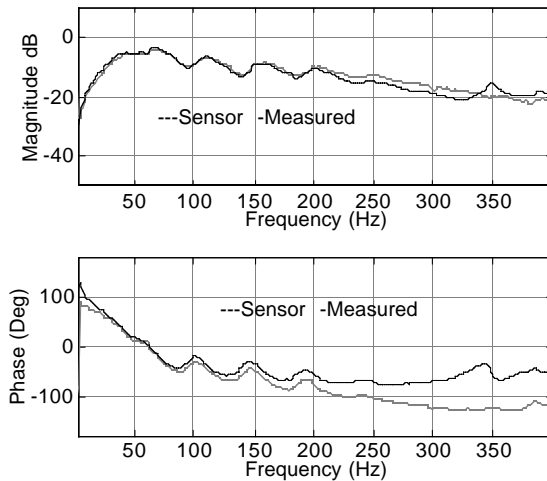


Figure 9: Comparison of Measured, Modeled and Sensor Model Speaker Velocity for Coupled Speaker/Duct System

Figure 9 shows that the good agreement between the measured velocity and the velocity sensor below approximately 200 Hz. There is less than 4 dB magnitude and 20 degrees phase difference between the two responses. There is significant phase error above 200 Hz. This error is attributed to the inductance effects in the speaker which become significant at high frequencies and which are not included in the velocity sensor.

Velocity Feedback Compensation of Speaker

The velocity feedback compensation strategy was then applied to the coupled speaker/duct system. The proportional gain, K_p , was varied from 0 to 100; and the measured velocity to desired velocity transfer function was measured from 0 - 200 Hz using the signal analyzer. Figure 10 shows that the measured speaker velocity response approached the desired velocity as the gain was increased. The noticeable deviation between the velocity sensor and the measured velocity may contribute to the 45 degree phase error above 100 Hz in the closed-loop system.

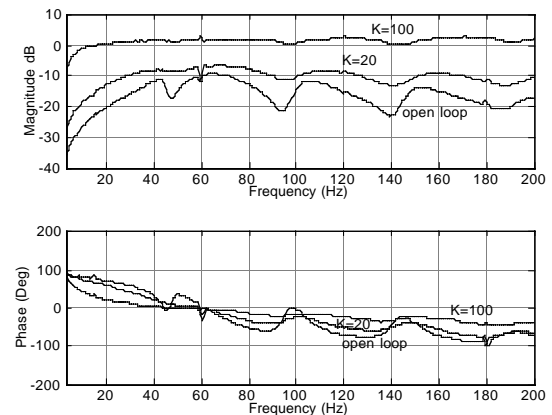


Figure 10: Comparison of Closed-Loop Speaker Velocity to Primary Speaker Voltage Frequency Response for Open Loop and Proportional Gains of 10, 20, and 100

The magnitude and phase variations exhibited in open-loop have been minimized. The effect of the duct resonances and the free-air resonance of the speaker are significantly reduced. With a value of

$K_p = 100$ there is less than 5 dB and 45 degrees magnitude and phase variation compared with 30 dB and 180 degrees in the uncompensated system. The compensated speaker velocity is independent from the speaker and duct dynamics. This response is ideal for an acoustic actuator.

CONCLUSIONS

This paper addresses using a compensated audio speaker as an actuator for systems with strong dynamic pressure coupling. It was shown that the response of an actuator is degraded by both the internal dynamics of the actuator and the interaction with the plant. Previous solutions are not effective for such applications because they only compensate for internal dynamics and not the pressure interactions from the plant. A new velocity sensor which uses a combination of speaker cone motion induced secondary coil voltage and primary coil current is developed and applied in proportional feed-back controller. An acoustic duct is used as an example of a system with strong dynamic pressure interactions. It is demonstrated through modeling and experiment that the compensated speaker response minimizes the effect of both internal actuator dynamics and coupling through the pressure with the acoustic plant.

The work presented here represents an ideal actuator whose design is independent of the acoustic plant, and unaffected by the dynamics of the plant. The compensation yields a feasible actuator for acoustic systems with strong pressure coupling.

REFERENCES

- Birdsong C.B., Radcliffe C.J., 1996, "A Compensated Actuator for an Acoustic Duct", Masters Thesis, Michigan State University.
- Bradley, P., 1995, "Active Assault on Cabin Noise", Commercial Aviation vol 77, September, 6 pp.
- Doak, P. E., 1973, "Excitation, Transmission and Radiation of Sound From Source Distributions in Hard-Walled Ducts of Finite Length (I): The Effects of Duct Cross-Section Geometry and Source Distributions Space-Time Pattern," Journal of Sound and Vibration, v 31, n 1 pp1-72.
- Hull A. J., Radcliffe C. J. Southward S. C., 1993, "Global Active Noise Control of a One-Dimensional Acoustic Duct Using a Feedback Controller" Journal of Dynamic Systems, Measurement, and Control, vol 115, September.
- Hull A. J., Radcliffe C. J., 1990, "State Space Representation of the Nonself-Adjoint Acoustic Duct System," Journal of Vibration and Acoustics v 112, October.
- IEEE Standard 219-1975, IEEE Standard Committee of Acoustics, Speech, and Signal Processing Group, "IEEE Recommended Practice for Loudspeaker Measurements", IEEE std. 219-1975.
- Karnopp, D. C., D. L. Margolis, and R. C. Rosenberg, 1990, "System Dynamics: A Unified Approach", New York, John Wiley & Sons, Inc.
- Radcliffe C. J., Gogate, S. D., 1996, "Velocity Feedback Compensation of Electromechanical Speakers for Acoustic Applications", International Federation of Automatic Control, Triennial World Congress, July.
- Radcliffe C.J., Gogate S.D., Hall G., 1994, "Development of an Active Acoustic Sink (AAS) for Noise Control Applications", Active Control of Vibrations and Noise, ASME.
- Radcliffe, C. J., Gogate, S. D., 1992, "Identification and Modeling Speaker Dynamics for Acoustic Control Applications", ASME Symposium on Active Control of Noise and Vibration.

Rough, W. J., 1996, "Linear System Theory", New Jersey, Prentice-Hall, Inc.

Seto, W. W., 1971, "Theory and Problems of Acoustics", New York, McGraw-Hill Book Company.

Spiekerman, C. E. and Radcliffe, C. J., 1986, "One-Dimensional Acoustic Response with Mixed Boundary Condition: Separating Total Response into Propagating and Standing Wave Components," Doctoral Dissertation, Michigan State University.

Warner, J., 1995, "Active Noise Control in an Off-Road Vehicle Cab" Noise and Vibrations Worldwide, vol 26 n, 7 July.